Development of barium boron aluminosilicate glass sealants using a sol–gel route for solid oxide fuel cell applications

J. Puig[1] · F. Ansart[1] · P. Lenormand[1] · R. Conradt[2] · S. M. Gross-Barsnick[3]

Abstract A key problem in the fabrication of planar solid oxide fuel cells is the sealing of the metallic interconnect to the ceramic electrolyte. The sealing material must be gas-tight, stable in different atmospheres at high temperature, chemically compatible with the other cell components and resistant to thermal stresses. Glass ceramic sealants are good candidates because of their high mechanical properties and the possibility to use a wide range of chemical compositions to control some physical properties like viscosity or coefficient of thermal expansion (CTE). In this work, glass sealants were synthesized using a sol gel route, which generally allows to obtain both homogeneity at a nanoscale and reduction of the processing temperature. The studied glasses were based on the system BaO B_2O_3 Al_2O_3 SiO_2 with varying amounts of CaO and MgO additions. Dilatometry, differential thermal analysis and hot-stage microscopy were the techniques used to determine optimal thermal treatment for sealing operation (880 °C with a dwell time of 10 h). The thermomechanical properties of the sealants were improved after sealing by a thermal treatment transferring the sealant into a favourable partially polycrystalline state. Gas-tightness tests performed after joining and 100 h ageing treatment at 800 °C under air of steel-sealant-steel assemblies highlighted that 4 of the selected glass chemical compositions remained impermeable. Joining degradations, crystalline phases evolution and CTE of these glasses were analysed. Electrical resistivities were larger than 10^5 Ω cm at 700 °C. On the basis of these results, four glasses were identified as promising candidates for this application.

Introduction

Solid oxide fuel cells (SOFCs) are great candidates to improve the performances of energy systems because of their high energy conversion efficiency. These cells allow a direct conversion of chemical energy of a redox reaction into electrical energy. The reactants are the air and hydrogen (or methane) and the main product is water. Individual cells are connected together in series to form stacks, which allow achieve high voltage outputs. These stacks have a great potential for power generation either in stationary or mobile applications and must work in the range 500 800 °C [1, 2].

In actual planar SOFCs studies, one of the challenges is concentrated on the development of sealants to ensure gas-tightness of cathodic and anodic compartments at high temperature (until 800 °C). These separating materials avoid the mixture of reactant gases, which prevent a decrease of efficiency in the production of electric energy. The sealant need to seal the adjacent cell components and

✉ J. Puig
jean.puig@promes.cnrs.fr

F. Ansart
ansart@chimie.ups tlse.fr

P. Lenormand
lenorman@chimie.ups tlse.fr

R. Conradt
conradt@ghi.rwth aachen.de

S. M. Gross Barsnick
s.m.gross@fz juelich.de

[1] CIRIMAT, Paul Sabatier University, 118 route de Narbonne, 31062 Toulouse, France

[2] GHI, RWTH Aachen, Mauerstrasse 5, 52064 Aachen, Germany

[3] Forschungszentrum Juelich GmbH, Wilhelm Johnen Strasse, 52425 Jülich, Germany

must be stable over long-term cell operation. An example of the design of a serial repeat unit used in stacks at the Forschungszentrum Jülich (FZJ) is given in Fig. 1 [3]. Three layers of glass ceramic are present in this figure: sealing the metal frame to the anode side of the interconnect plate, sealing the metal frame to the cathode side of the interconnect plate, and sealing the cell outer rim to the interconnect plate [3, 4].

The most important physico-chemical properties of the sealant material are high temperature stability, high electrical insulation ($10^4 \, \Omega$ cm), gas-tightness, good adhesion between steel and electrolyte, thermal expansion stability with a coefficient of thermal expansion (CTE) close to other cell components ($10\text{–}13 \times 10^6 \, K^{-1}$), chemical stability in reducing and oxidizing atmospheres with no reaction product at the interface with other cell components and a sufficient plasticity at the joining temperature [5]. A great number of sealant materials and approaches have been investigated, for this application, such as glasses, glass ceramics, glass ceramic composites and cements [6, 7]. Among the most promising materials, glass ceramic sealants have been extensively studied for this application because of their good mechanical, chemical and electrical insulation properties and the possibility to use a wide range of chemical compounds to control physical properties such as viscosity or CTE [6, 8].

Among the glass ceramics, barium silicate glasses had been extensively developed with a lot of investigations on the influence of various additives on the glass ceramics properties [8–16]. These compositions result in partially crystallized materials with a relatively large glassy phase volume. The barium silicate phases crystallize in all glasses, while other phases can be promoted or inhibited as a function of additive elements. For instance, increasing the BaO content and the B_2O_3/SiO_2 ratio in a glass chemical composition allowed an increase of the CTE of glasses [9]. The addition of B_2O_3 produces an expected decrease of viscosity and delay in the crystallization. These phenomena lead to a greater wettability of the glasses on the steel, but B_2O_3 content must be quite low because of the formation

of volatile compounds at high temperatures [10]. At a first glance, small additions of CaO, MgO, Y_2O_3, La_2O_3 and ZrO_2 seemed to have little impact on the thermomechanical properties of glass ceramics [10]. Nonetheless, with an ageing of 200 h at 900 °C, devitrification of glass ceramics are more advanced and different crystal phases appear in bulk glass. Some crystals cause a decrease of the glass ceramics' CTE, which can lead to a mismatch with the CTE of other cell components [11]. On the contrary, barium silicate crystal phases like $BaSiO_3$ (needle shaped) have high CTE varying from 12.7 to $19 \times 10^{-6} \, K^{-1}$ [11, 12]. Another problem of devitrification is the formation of monocelsian $BaAl_2Si_2O_8$ with a low CTE during ageing operation. A good example of unfavourable phase formation during SOFC working conditions is observed in the G18 glass developed by researches of Pacific Northwest National Laboratory (PNNL). Under SOFC operation conditions, with temperatures between 750 and 850 °C, the G18 glass already after 1 h shows the presence of monocelsian crystalline phase [13]. Due to the formation of monocelsian, the CTE of this glass is 15 % reduced after 168 h under operation conditions. The CTE reduction is stabilized after 336 h at 750 °C, as the crystallization stops. Barium silicate glasses showed severe reactions at the steel glass interface with the formation of an undesirable phase $BaCrO_4$, provoking an increase of the sealant CTE [14–17]. Metal rich nodules had already been observed at this interface giving rise to local short-circuiting effects which probably results in stack failure [18, 19]. The formation of these nodules was observed and explained by Haanappel and al. [20]. Therefore, the type of the steel is also a critical parameter in avoiding reactions with the glass ceramics.

The development of new low BaO content or Ba-free glasses was motivated by the interest in decreasing or avoiding these chemicals interactions with the interconnector steel. Improvements were noted with the Ba-free SALST and SALSZT (SiO_2 Al_2O_3 La_2O_3 SrO ZnO TiO_2) glasses. These glass compositions were able to successfully seal GDC ($Gd_{0.2}Ce_{0.8}O_{2-\delta}$) ceramic electrolyte and SUS430 stainless steel assemblies with good thermal stability and low gas-leakage rate during 500 h at 700 °C [21]. Smeacetto et al. showed that alkali Ba-free glass called SACN (SiO_2 Al_2O_3 CaO Na_2O) presented good wettability on both substrates of the assemblies that were 8-YSZ (8 mol% yttria stabilized zirconia) electrolyte and various types of interconnector steels, i.e. Crofer22-APU and AISI430 [22, 23]. The disadvantage of low BaO or Ba-free glasses is the decrease of CTE compared to the Ba-rich glasses. However, the lower CTE glasses would not be suitable for certain types of steel, i.e. K41X (high CTE of $13 \times 10^{-6} \, K^{-1}$), which has been used in the present study.
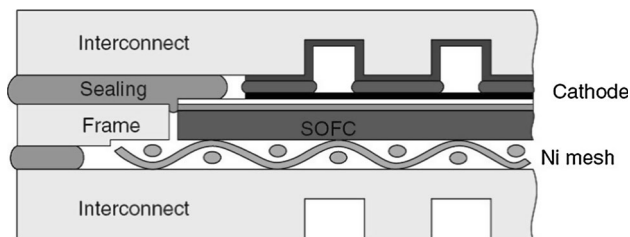

Fig. 1 Schematic presentation of a repeating unit of a planar SOFC with a rigid glass ceramic seal [3]

Another kind of glass sealants is also developed in order to better tolerate the CTE mismatching. Contrary to the rigid glass ceramic sealants, these viscous sealants retain the softening behaviour of glasses to relieve stresses, that enable to prevent damages that occur during thermal cycling of the cells. Compliant borosilicate glasses with or without alkaline compounds had already been tested and appeared to be new interesting materials as glass sealant for SOFC application [24, 25].

Taking into account all the state-of-the-art, this study propose a new nonconventional process based on soft chemistry techniques. Few authors have shown that the synthesis by sol gel route of barium aluminosilicate compounds was feasible [26, 27]. With the proposed glass processing technique by sol gel, an important point for the SOFC development can be achieved: cost reduction because the sealant materials are processed by sol gel route at lower temperatures. Many studies showed that the use of gel mixtures could decrease the temperature of glass formation until 200 K below (possibly more) those required when using conventional batch material [26, 28]. By this process, the reduction of the process temperature is possible due to a better homogeneity of the cationic salts mixture compared to solid-state routes (macroscopic mixture of simple oxides). Another positive argument is that the reached homogeneity could induce better materials properties and increase lifetime.

A novel synthesis of barium (magnesium) aluminosilicate glasses (rigid sealants) using the sol gel route had been recently established in a previous work [29]. Tetraethyl orthosilicate (TEOS) and aluminium-tri-sec-butoxide (ASB) were mixed together in a first step following by the addition of barium and magnesium acetates (pre-diluted in water). After gelation and drying, homogeneous xerogels were obtained. These gels were treated thermally to form glass ceramics at 1150 1300 °C. However, various crystals were formed in these glasses [29].

In the present study, some new compounds like B_2O_3 and CaO have been added to directly form homogeneous glasses. The selected glasses have chemical compositions with high BaO content, close to the previous G18 glass [13] and could be used as sealant materials in SOFCs working at 700 800 °C. Thermal properties of glasses as-formed and of glass ceramics after joining and ageing (thermal treatment) under air were investigated. Crystalline phase evolution and expansion of glasses were studied to evaluate stability of glass ceramics during this treatment. Leakage tests and electrical resistivity tests were carried out on steel sealant steel assemblies to confirm potential candidates for this application.

Materials and methods

Synthesis of glass–ceramics by sol–gel route

Glass ceramics were synthesized using a new sol gel alkoxide route followed by a thermal treatment at 1300 °C (Fig. 2). Silicon and aluminium alkoxides (TEOS and ASB) were mixed together in order to form a homogeneous solution during the first and the second step of the chemical procedure as it was previously described [29]. At the third step of the chemical procedure, acetate salts and boron oxide were added to the mixture in order to obtain BaO B_2O_3 X = MgO, CaO Al_2O_3 SiO_2 (BBXAS) glasses. After one gelation day, xerogels remained translucent (white colour; Fig. 2) and no phase separation was observed. A better homogeneity in the cationic salt mixtures as compared to solid state or melting routes (macroscopic mixture of simple oxides) is expected, which will be checked in a future study. Multi-oxides powders BBXAS, observed with SEM after calcinations at 850 °C 4 h, exhibit a nanometric grain size. After a processing temperature of 1300 °C during 2 h, followed by a glass casting on graphite plates at ambient temperature (cooling rate >1000 K min^{-1}), homogeneous glasses were obtained. No crystalline phases were identified by scanning electron microscopy with field emission gun (FEG-SEM) or X-ray diffraction (XRD).

Different parameters such as alkoxide/solvent ratio, temperature and time between every step, hydrolysis ratio $W = [H_2O]/[TEOS]$ and complexation ratio $R = [CH_3COOH]/[TEOS]$ were optimized to obtain homogeneous gels (Table 1).

An identical glass processing temperature was fixed at 1300 °C for all samples in order to compare glasses with the same protocol. Nevertheless, lower glass processing temperature could be used to obtain homogeneous glasses by sol gel route. As an example, CM2 glass could remain homogeneous after a glass processing at 1150 °C during 2 h.

Five different chemical compositions were prepared to evaluate influences of CaO and MgO on sol gel glasses properties (Table 1). ICP-AES experiments revealed that the chemical composition of glasses made by this soft process was close to theoretical compositions (comparable with the results attained by a conventional melting process). BaO content was a little higher and SiO_2 content made the balance, which created glasses with a lower silica content than expected for the intended chemical compositions. The analytical error of ICP-AES (SCA, Solaize) is about 1 10 % for elemental concentrations below 5 mol%.

Glasses were ground using a planetary mill (agate balls and cup) to obtain powders. Grain sizes were determined
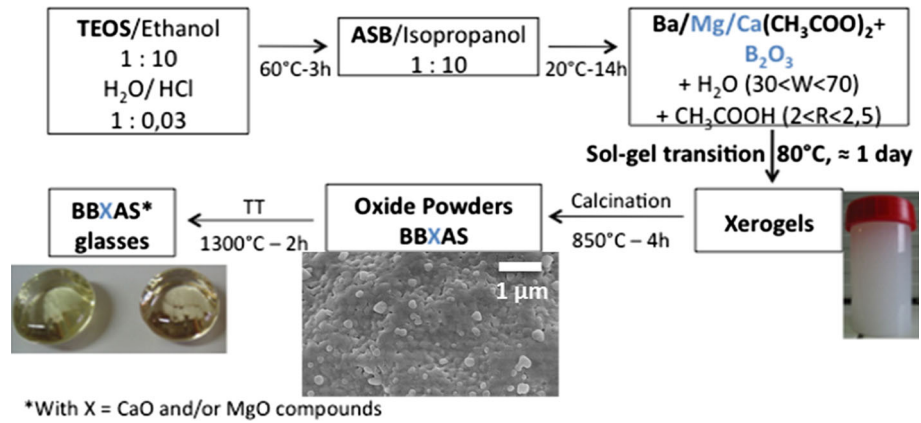
Table 1 Chemical compositions of glasses checked by ICP AES

Glasses	Synthesis parameters		Theoretical compositions (mol%)						Real compositions by ICP AES (mol%)					
	W*	R**	BaO	Al_2O_3	B_2O_3	MgO	CaO	SiO_2	BaO	Al_2O_3	B_2O_3	MgO	CaO	SiO_2
C1	70	2	36	2.6	10.3	0	10.3	41	39.1	2.7	9.8	0	10.5	38
C2	70	2	36	2.6	10.3	0	15.4	35.8	38.2	3.1	9.5	0	15.3	33.8
CM1	70	2.5	36	2.6	10.3	5.1	10.3	35.8	36.9	3	9.4	5.5	10.5	34.7
CM2	70	2.5	36	2.6	10.3	10.3	10.3	30.7	36.7	2.8	9.6	10.4	10.7	29.9
M2	60	2.5	36	2.6	10.3	15.4	0	35.8	36	2.6	9.9	16.1	0	35.4

* Hydrolysis ratio W $[H_2O]/[TEOS]$

** Complexation ratio R $[CH_3COOH]/[TEOS]$

by a laser diffraction method, using a Beckman coulter LS particle size analyzer (LMTG laboratory, Toulouse). All the powders were polydisperse with a median grain size in volume between 16.3 and 19.3 μm. The grain size was smaller than 70 μm, which was suitable to seal SOFC components.

Characterization methods

Crystallization kinetics of the BBXAS glass powders were analysed using a simultaneous differential thermogravimetrical analysis (DTA) Netzsch STA 409 C/CD system coupled with a computerized data acquisition and analysis system. 100 mg of each glass powder was contained in alumina crucible. Scans were also recorded from room temperature to 1100 °C at 10 K min^{-1}. T_g (transition temperature), T_x (onset crystallization temperature) and T_c (maximum crystallization temperature) of each glass were recorded.

Measurements of CTE as a function of temperature were carried out on bulk glass pellets 6 mm in diameter and 2 mm thick using a dilatometer with a sensor Setsys Evolution TMA. CTE values were calculated between 200 and 550 ° C under air atmosphere; three pellets of each

chemical composition were characterized. Relative errors of the calculations were in the range 5 6 %. Scans were recorded from room temperature to 1100 °C at 10 K min^{-1}.

Hot-stage microscopy measurements (HSM) were performed using a Hesse Instrument EMI1 equipment, which is composed of a CCD camera and a heat controlled furnace. Each glass powder was pressed into a pellet ($\sim$3 mm height $\times$ 3 mm diameter) and samples were heated at 10 K min^{-1} from room temperature to 1100 °C on standard platinum substrate. Images were recorded at 10 K min^{-1} intervals. Sample morphologies and contact angles were determined by a computer program, according to the norm DIN 51730 1998-04 (testing of solid fuels determination of fusibility of fuel ash) to calculate T_{FS} (first shrinkage), T_S (softening), T_{SP} (sphere), T_{HB} (half-ball) and T_F (flow) of each glass formulation. T_{MS} (maximum shrinkage) was estimated by a graphical method which had already been used in HSM studies. Three samples of each chemical composition were analysed to have a reasonable average on calculations.

In order to investigate the joining properties, sandwiched samples of two 1.5 mm thick plates of ferritic steel K41X with the size of 50 $\times$ 50 mm^2 were joined

with the glasses. One of the steel squares had a drill hole of 10 mm in the middle of it, which allows the performance of helium leakage test. The steel K41X (from Arcelor) is a low cost material with a high chromium content (17.8 wt%) to use it at 700 800 °C. Small additions of Si, Nb, Ni and Mn were included in K41X (less than 2 wt%). Surfaces of steel plates were first cleaned with ethanol. This standard joining sample setting was established earlier by Gross et al. [30].

For the application of the glass, the powder was blended to a paste, using ethyl cellulose as binder in terpineol. The paste was then dispensed by robot tracking to the steel surface. The joining of the sample was carried out by placing a dead load of 400 g on top of the second steel plate and heating-up in a resistance heated chamber furnace in air. The same heat treatment was used in accordance with the thermal analysis results for all the glass samples. Constant heating and cooling rates of 2 K min^{-1} were used for all the joining experiments. An ageing process was also performed in order to evaluate the evolution of the sealant in operating temperature after the first 100 h.

Gas-tightness was checked by helium leakage detection (UL200, Inficon) at a difference in pressure of 1000 mbar. The sandwich sample was adapted with the drill hole side to a vacuum pump and a mass spectrometer allowed to obtain the He-leakage rate using the equation:

$$q_L = \Delta(p \cdot V)/\Delta t, \tag{1}$$

where q_L is the leakage rate; p is the pressure or pressure variation in (mbar); V is the volume or volume variation in (l) and Δt is a time period in (s). Due to the units from the parameters used in the leakage rate calculation, the leak rate is expressed in mbar l s^{-1} [31].

The sample cross-sections were analysed by FEG-SEM, model JEOL JSM 6700F, coupled with energy dispersive X-ray detector (EDX). Microstructure analysis was used to determine both the size and morphology of the crystals as well as to investigate the chemical reactions occurring at the interface between glass ceramics and steel in the joining samples during sealing and ageing procedure.

The crystalline structure of glass ceramic pellets (6 mm × ~2 mm) was analysed using XRD technique after thermal treatments simulating sealing and ageing operations. XRD equipment was a Brucker AXS D4 Endeavor. Scans were recorded between 10° and 100° operating in Bragg Brentano (θ 2θ) mode.

Before the electrical tests, a pellet of each glass ($\varnothing \approx 6$ mm, height ≈ 4 mm) was used to seal two parallel K41X steel square plates of 1 cm^2 at 850 °C during 2 h. Electrical measurements were performed at 700 °C on these assemblies with an electrical impedance spectrometer material mates. Resistivities of steel plates were negligible (<1 Ω cm at 700 °C).

Results and discussion

After the glass processing at 1300 °C, all the materials were amorphous. No diffraction pattern was detected using XRD, and no crystals were observed using SEM (see Fig. 3a, b; small blank points correspond to dust on the glass surface). Considering micrographs, no phase separation was detected. So, all the glasses were homogeneous.

In general, the glass transition is the first criterion to be taken into account because glasses have a visco-elastic behaviour above this temperature. Considering SOFC applications, the barium silicate glasses have general T_g between 575 and 685 °C [9, 10, 13, 15]. The five glasses synthesized using a sol gel process had T_g values close to the lower values of this range (Table 2). In particular, the chemical composition of glass C2 was close to glass G18 [13]. Consequently, the T_g of C2 was close to the T_g of G18 already described in literature: 615 versus 630 636 °C cited for G18 [10, 13].

In the five glasses produced in this work, the B_2O_3/SiO_2 ratios varied in between 0.26 and 0.32 with a similar SiO_2 content for most of them, except for CM2 which had a bit lower silica content. This could explain the quite similar T_g for all the glasses studied.

For a glass sealant, CTE at its best should be in the range between coefficients of thermal expansion of the steel used, in this case the K41X is 12.9 × 10^{-6} K^{-1}, and of the electrolyte, for example, the 8-YSZ is close to 11 × 10^{-6} K^{-1}. The measured CTE of the as-formed glasses studied in this work were in the range of 12.2 13.9 × 10^{-6} K^{-1} (Table 2). Glasses CTE increases with CaO content. For instance, C2 contained 5 mol%. CaO more than C1 and has coefficient 1.7 × 10^{-6} K^{-1} higher than the C1 glass. Nevertheless, in glasses containing CaO and MgO, the CTE appeared more stabilized. The CTE of C1, CM1 and CM2 could be classified in the following order: C1 < CM1 ~ CM2, proving that there may exist a threshold in mixing CaO and MgO oxide in glasses in order to increase the CTE.

During the devitrification process, glasses containing MgO formed low CTE magnesium silicates crystals like cordierite. For all the glasses in this work, another devitrification problem could be the formation of monocelsian crystals $BaAl_2Si_2O_8$ with a very low CTE of 2 3 × 10^{-6} K^{-1} [11]. All these considerations could lead to an important increase or decrease of the CTE of glass ceramics formed during a thermal treatment, which allows arguing that it is not possible to select them as an ideal seal basing on this criterion alone. Dilatometry experiments of the glass ceramics sintered using the same thermal treatment as in the joining process and aged treatments have been shown in the following results in order to observe thermal operations effects on CTE evolution.
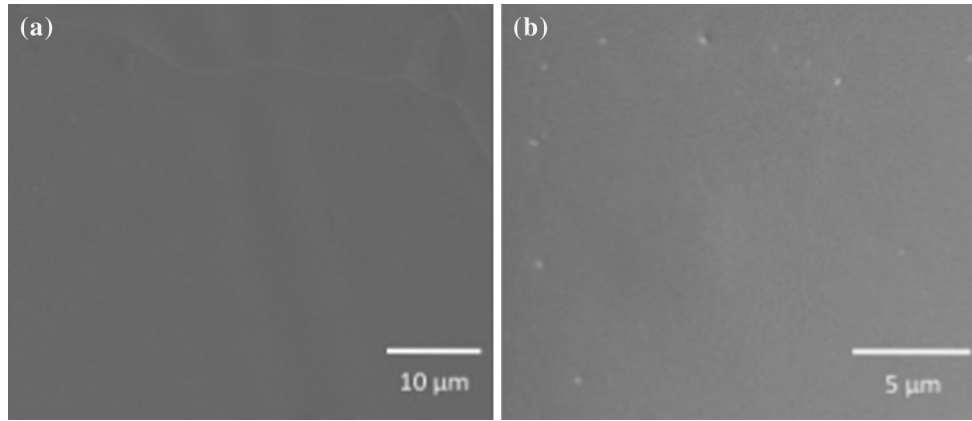
Fig. 3 SEM backscattered micrographs of **a** M2 and **b** CM2 as formed glasses

Table 2 Characteristic temperatures of as formed glasses using DTA and HSM. CTE were measured by dilatometry technique

Glasses	T_g (°C)	T_{MS} (°C)	T_S (°C)	T_x (°C)	T_c (°C)	T_{HB} (°C)	CTE ($\times 10^{-6}$ K^{-1})
C1	626	720	744	710	803	911	12.5
C2	615	702	725	722	783	921	14.5
CM1	612	725	727	708	800	907	13.0
CM2	596	690	705	706	793	948	12.9
M2	608	704	703	710	784	974	13.6
Measured σ	±2	±10	±16	±2	±2	±11	±0.3

Fig. 4 Rheological behaviour of a CM1 glass pellet versus temperature with HSM from ambient temperature to flow temperature T_F (the shape of the glass pellet at T_{MS} is often similar to T_S)
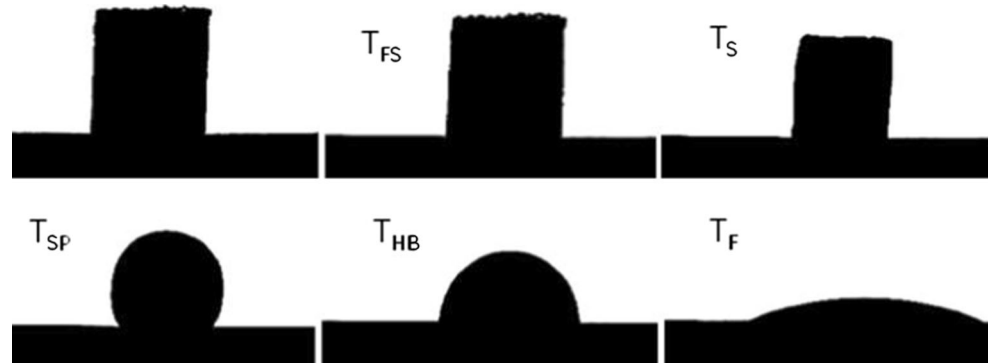
An example of the rheological behaviour of CM1 glass powder samples (pressed in a pellet form) is shown in Fig. 4. All of the five glasses had a similar rheological behaviour from ambient temperature to T_S, i.e. samples shrunk and began to soften.

At the maximum shrinkage temperature T_{MS} (Table 2; Fig. 5), glasses reached the maximum density. T_X of C2, CM2 and M2 are greater or equal to the respective T_{MS}, which shows that crystallization phenomenon started soon after the sintering process. T_X of the two other glasses was slightly inferior to the corresponding T_{MS}. Considering that the error on T_{MS} was high (±10 K), sintering and crystallization steps were considered as independent phenomena.

Therefore, porosity problems were supposed to be avoided in a high density material.

The calculated error (σ) on T_{SP} and on T_F was very high for the glass samples (respectively, ±40 and ±65 K). So, these results were not presented in order to simplify the analysis. Furthermore, the HSM software could not calculate T_{SP} values for M2 and CM2 glass samples. A hypothesis is that the formation of crystals may inhibit the evolution of the sphere point by mechanical strain. This problem may reveal a stronger devitrification in CM2 and M2 glasses, which had higher MgO contents. By contrast, temperatures T_{HB} were determined at a reasonable precision and were considered as more reliable data to
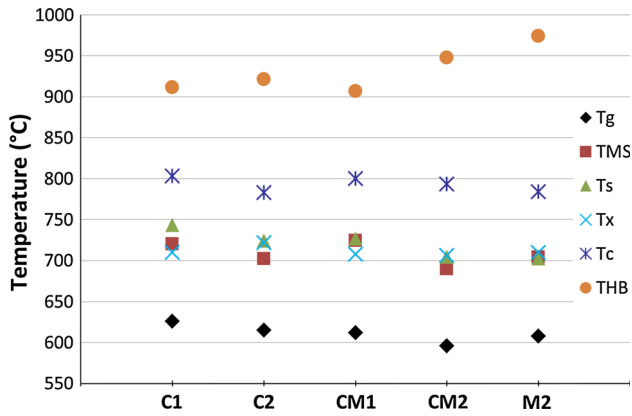
Fig. 5 Main characteristic temperatures of glasses evaluated by DTA and HSM

Fig. 6 Backscattered electron micrographs of polished cross sections of M2 glass on steel after sealing operation (880 °C 10 h)

determine the future joining temperature. T_{HB} of M2 and CM2 are high because of the probable formation of crystals, which could slow the deformation of glass samples during heat treatment (Table 2).

In order to obtain a rigid seal with high mechanical properties, it is necessary to have strong devitrification in glasses. So, sealing temperature must be higher than T_c to obtain a glass ceramic with a high crystallized content. An intermediate viscosity is appropriate to ensure cell integrity. Furthermore, the T_J (joining temperature) must be lower than T_{HB} to avoid glass flow. Consequently, the T_J must be in the range (T_c T_{HB}). When the contact angle is high, a pressure could be applied to facilitate joining [9]. Considering these essential facts, and in order to compare glasses at a similar sealing temperature, a unique T_J of 880 °C was chosen.

Steel sealant steel assemblies were sealed using a joining temperature of 880 °C during 10 h and with a dead top load (400 g).

He-leakage results are shown in Table 3. The sealants for SOFCs are considered to be gas-tight with a He-leakage rate of 10^{-7} mbar l s^{-1} [8, 31].

Assemblies containing C1, C2, CM1 and CM2 glass ceramics were tight with He-leakage rates smaller 10^{-8} mbar l s^{-1}. The sample joined with M2 sealant was not tight after the joining treatment. Further investigations showed that this sample had big pores, which can be the reason for the untightness (Fig. 6). Considering that T_{SP}
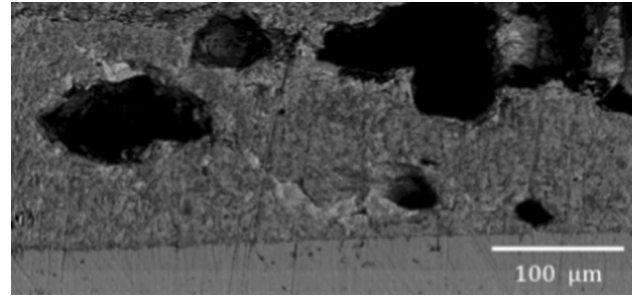
could not be calculated by the software because of a presumed strong crystallization and that T_{HB} is very high (974 °C), it is possible that the joining temperature used for the sealing procedure of steel M2 glass steel assembly was not high enough. This glass was found not suitable for the chosen SOFC application because a high joining temperature could be harmful for K41X steel.

The composition M2 was not aged because of the non-satisfactory result as joined. All the assemblies were gas-tight after ageing operations at 800 °C during 100 h (Table 3). Post-mortem analyses confirmed that the four remaining glasses adhered to steel and that the chosen T_J was adequate (Fig. 7). The thicknesses of the glasses were around 100 500 μm. No cracks at the interfaces and within the materials were detected. The relatively rough appearance of the interfaces was due to the applied mechanical polishing.

Devitrification was particularly strong in CM2 and M2 glasses. Different shapes of crystals were observed in glass ceramics (Fig. 7): especially, white crystals possibly corresponding to $BaSiO_3$ (or other barium silicates like $Ba_2Si_3O_8$), blocky grey crystals possibly identified as barium calcium silicate crystals and little needle-shaped crystals containing magnesium and silicon (probably $MgSiO_3$) [11, 13]. Elemental dispersive X-ray analyses proved that no diffusion of elements between glasses and steel occurred.

$BaCrO_4$ was not identified at the glass-steel interface after 100 h of heat treatment although this phase was present in other similar studies using barium aluminosilicate glasses [13, 15, 20]. No hexacelsian phase (very thin

Table 3 Helium leakage results on steel glass ceramics steel assemblies

Samples	Sealing operation (mbar l s^{-1}) 880 °C 10 h	Ageing operation (mbar l s^{-1}) 800 °C 100 h
C1	1.0E 09	4.0E 08
C2	1.0E 08	1.0E 08
CM1	1.0E 09	2.0E 08
CM2	1.0E 08	1.0E 08
M2	Untight	

Fig. 7 Backscattered electron micrographs of polished cross sections of glass K41X interfaces after an ageing operation of 800 °C   100 h with: **a** C1, **b** C2, **c** CM1, **d** CM2
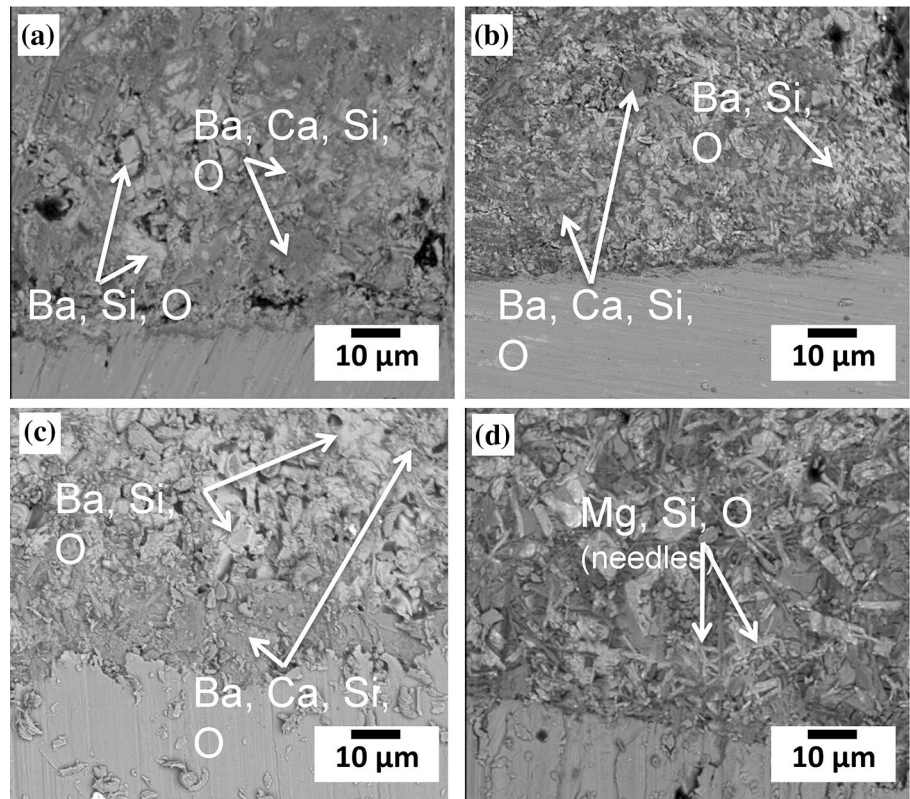

needle-like dark crystals) was observed in the aged glasses. Thus, no monocelsian crystals with low CTE were supposed to be formed.

XRD technique was used to identify the crystalline phases on the four promising materials (C1, C2, CM1 and CM2 glasses) after a simulated sealing operation at 880 °C during 10 h (Fig. 8a). $BaSiO_3$ and $Ba_{0.9}Ca_{0.1}SiO_3$ were the major phases in C1, C2 and CM1 glass ceramics, which confirmed previous microstructure observations. Barium silicates and barium calcium silicates are generally the first phases to crystallize in BCAS glass [32]. These phases have high CTE (10.5 15.4 × 10^{-6} K^{-1}) [11], in the range expected for the synthesized materials. $MgSiO_3$ was the major phase in CM2 glass ceramic and was identified in CM1. This phase has a low CTE around 7 8 × 10^{-6} K^{-1},

which was supposed to decrease the CTE of CM1 and CM2 glass ceramics during devitrification. Further peaks were attributed to indexed barium silicates or barium magnesium silicates phases. CTE measurements (Fig. 9) confirmed that the CTE values of CM1 and CM2 glass were slightly reduced after the sealing procedure. The CTE of C1 and C2 glasses stabilized around 13 14 × 10^{-6} K^{-1} after the joining, certainly due to the barium calcium silicate and barium silicate crystals formation observed on Fig. 8a.

After an ageing treatment of 100 h at 800 °C, the same crystalline phases were identified in glass ceramics (Fig. 8b). No hexacelsian and monocelsian phases $BaAl_2$ Si_2O_8 were identified in the glass ceramics after sealing and ageing operations. According to literature, hexacelsian was present in several BCAS glasses after thermal

Fig. 8 Crystalline phases determined after different thermal treatments: **a** 880 °C   10 h, **b** 880 °C   10 h + 800 °C   100 h, using XRD technique
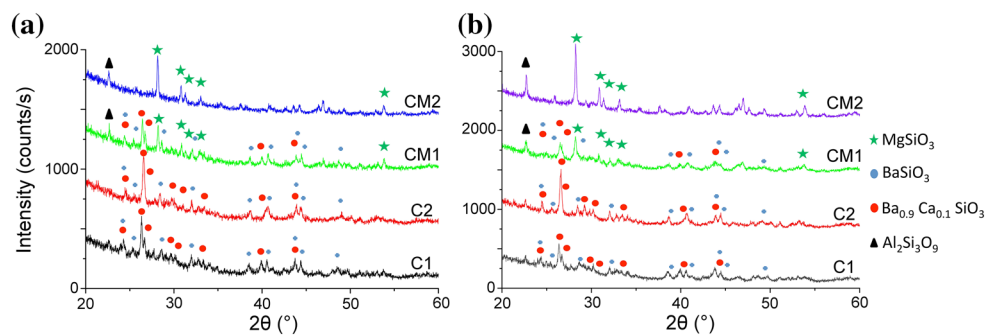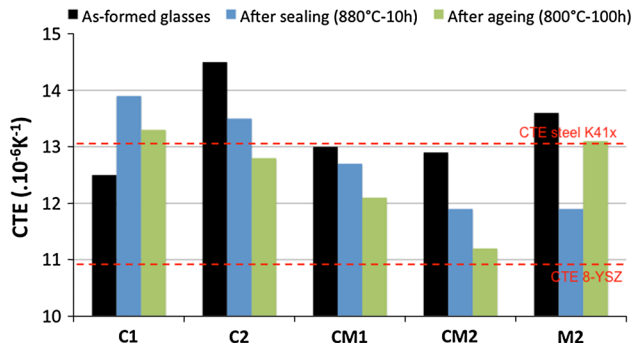
Fig. 9 Evolution of the CTE of glasses after sealing and ageing treatments

treatments of 10–100 h and could transform over time into monocelsian phase, which could degrade their thermomechanical properties [19, 32, 33]. The absence of this phase could be due to the weak Al_2O_3 content in as-formed glasses and/or to a preferred crystallization of other crystalline phases induced by homogeneity of glass powders obtained using the sol–gel process.

CTE of glass ceramics is slightly reduced after the ageing treatment of 100 h at 800 °C, which proved their thermal stability. Therefore, thermomechanical and structural properties were well correlated, which argue positively on a long-term stability of the four glasses. In particular, CTE of CM1 and CM2 remained between CTE of the sealed steel K41x interconnector and 8-YSZ electrolyte after all the heat treatment.

In order to avoid shunting, the electrical resistivity of a glass sealant should be larger than 10^4 Ω cm [8]. All the measured resistivities were above the fixed threshold from 10^5 to 10^6 Ω cm (Table 4). The assembly with M2 glass was broken after the sealing treatment probably due to the numerous pores previously observed in this glass (Fig. 6); thus, the resistivity value of this material could not be measured.

Glass–ceramics synthesized in this study (except M2 glass) exhibit lower resistivities than conventional BaO–MgO silicate glasses (10^8 Ω cm [34]) due to the high amounts of BaO and B_2O_3 content. Differences in resistivities values between the four devitrified glasses could be correlated with CaO and MgO contents. C1 had the lower content of both oxides and exhibited the highest resistivity. The resistivity decreased with more CaO (C2) and more magnesium (CM1 and CM2)

replacing SiO_2. Ca^{2+} and Mg^{2+} ions have a low ionic radius and are supposed to be transported more easily in the glass ceramics, which can cause an increase of conductivity. The weak difference in electrical resistivity between CM1 and C2 could be explained by the fact that Mg^{2+} has a lower ionic radius than Ca^{2+}. Indeed, it had been already proved that a lower ionic radius from an additive oxide decrease electrical resistivity of a Barium silicate [35]. Therefore, electrical measurements were well correlated with glass chemical composition and the measured values were suitable for SOFCs.

Conclusion

Glass materials within the system BBXAS (X = MgO, CaO) were developed using a new sol–gel route. Materials remained amorphous and homogeneous under a processing temperature of 1300 °C. The homogeneity in the cationic salts mixture obtained should be compared to solid-state route in further investigations in order to better understand the advantages of the sol–gel process. CTE values increased with increasing CaO and MgO content, except for the CM2 glass. However, these values remained close to the CTE of steel and electrolyte.

The study of the rheological behaviour of glasses allowed to select a unique joining temperature. Although the M2 glass ceramic was porous after the sealing treatment, the four other materials remained gas-tight even after ageing, and no reaction product was formed at the glass-steel interfaces after 100 h at 800 °C in air atmosphere. Furthermore, no hexacelsian or monocelsian was detected; structural and thermomechanical properties did not change significantly after the ageing operation. Electrical measurements proved that these materials were suitable electrical insulators at high temperature.

Considering all these results, C1, C2, CM1 and CM2 glasses were thermally and chemically stable after 100 h at 800 °C in air atmosphere, which makes them suitable candidates for SOFC applications at 700–800 °C (and maybe at lower temperature, i.e. 650 °C). Tests at high temperature under dual atmosphere (air/H_2) must be carried out over longer period (>1000 h) using these materials to confirm the promising results. Elaboration of viscous sealants using the sol–gel route is also planned in future experiments.

Table 4 Electrical resistivities of glass ceramics after a sealing operation of 850 °C–2 h

Samples	Resistivity (Ω cm)	Accuracy (Ω cm)
C1	1.0E+06	1.0E+05
C2	7.6E+05	5.0E+04
CM1	6.3E+05	5.0E+04
CM2	3.4E+05	5.0E+04

References

1. Steele BCH, Heinzel A (2001) Materials for fuel cell technologies. Nature 414:345–352

2. Haile SM (2003) Fuel cell materials and components. Acta Mater 51:5981 6000

3. Buchkremer HP, Conradt R (2010) Durable sealing concepts with glass sealants or compression seals. In: Vielstich W, Gasteiger HA, Lamm A, Yokokawa H (eds) Handbook of fuel cells: fun damentals, technology and applications. Wiley, Hoboken

4. Blum L, Gross SM, Malzbender J et al (2011) Investigation of solid oxide fuel cell sealing behavior under stack relevant con ditions at FZJ. J Power Sources 196:7175 7181

5. Mahapatra MK, Lu K (2010) Thermochemical compatibility of a seal glass with different solid oxide cell components. Int J Appl Ceram Technol 7:10 21

6. Fergus JW (2005) Sealants for solid oxide fuel cells. J Power Sources 147:46 57

7. Lessing PA (2007) A review of sealing technologies applicable to solid oxide electrolysis cells. J Mater Sci 42:3465 3476. doi:10.1007/s10853 006 0409 9

8. Mahapatra MK, Lu K (2010) Seal glass for solid oxide fuel cells. J Power Sources 195:7129 7139

9. Sohn SB, Choi SY, Kim GH, Song HS, Kim GD (2002) Stable sealing glass for planar oxide fuel cell. J Noncryst Solids 297:103 112

10. Flugel A, Dolan MD, Varshneya AK et al (2007) Development of an improved devitrifiable fuel cell sealing glass I. Bulk proper ties. Electrochem Soc 154:B601 B608

11. Dolan MD, Misture ST (2007) Development of an improved devitrifiable fuel cell sealing glass II. Crystallization behavior and structures of crystalline phases. Electrochem Soc 154:B700 B711

12. Kerstan M, Russel C (2011) Barium silicates as high thermal expansion seals for solid oxide fuel cells studied by HT XRD. J Power Sources 196:7578 7584

13. Meinhardt KD, Kim DS, Chou YS, Weil KS (2008) Synthesis and properties of a barium aluminosilicate solid oxide fuel cell glass ceramic sealant. J Power Sources 182:188 196

14. Goel A, Tulyaganov DU, Kharton VV, Yaremchenko AA et al (2009) Optimization of La_2O_3 containing diopside based glass ceramic sealants for fuel cell applications. J Power Sources 189:1032 1043

15. Ghosh S, Sharma AD, Mukhopadhyay AK, Kundu P, Basu RN (2010) Effect of BaO addition on magnesium lanthanum alumino borosilicate based glass ceramic sealant for anode supported solid oxide fuel cell. Int J Hydrog Energy 35:272 283

16. Yang Z, Stevenson JW, Meinhardt KD (2003) Chemical inter actions of barium calcium aluminosilicate based sealing glasses with oxidation resistant alloys. Solid State Ionics 160:213 225

17. Peng L, Zhu Q (2009) Thermal cycle stability of BaO B_2O_3 SiO_2 sealing glass. J Power Sources 194:880 885

18. Batfalsky P, Haanappel VAC, Malzbender J, Menzler NH et al (2006) Chemical interaction between glass ceramic sealants and interconnect steels in SOFC stacks. J Power Sources 155:128 137

19. Ghosh S, Sharma AD, Kundu P, Mahanty S, Basu RN (2008) Development and characterizations of BaO CaO Al_2O_3 SiO_2 glass ceramic sealants for intermediate temperature solid oxide fuel cell application. J Noncryst Solids 354:4081 4088

20. Haanappel VAC, Shemet V, Gross SM, Koppitz T, Menzler NH et al (2005) Behaviour of various glass ceramic sealants with ferritic steels under simulated SOFC stack conditions. J Power Sources 150:86 100

21. Wang SF, Hsu YF, Lu HC, Lo SC, Cheng CS (2012) B_2O_3 free SiO_2 Al_2O_3 SrO La_2O_3 ZnO TiO_2 glass sealants for interme diate temperature solid oxide fuel cell applications. J Int Hydrog Energy 37:5901 5913

22. Smeacetto F, Salvo M, Ferraris M, Casalegno V, Asinari P (2008) Glass and composite seals for the joining of YSZ to metallic interconnect in solid oxide fuel cells. J Eur Ceram Soc 28:611 616

23. Smeacetto F, Salvo M, D'Herin Bytner FD, Leone P, Ferraris M (2010) New glass and glass ceramic sealants for planar solid oxide fuel cells. J Eur Ceram Soc 30:933 940

24. Coillot D, Méar FO, Nonnet H, Montagne L (2012) New viscous sealing glasses for electrochemical cells. Int J Hydrog Energy 37:9351 9358

25. Hsu JH, Kim CW, Brow RK, Szabo J, Crouch R, Baird R (2014) An alkali free barium borosilicate viscous sealing glass for solid oxide fuel cells. J Power Sources 270:14 20

26. Tredway HK, Risbud SH (1988) Gel synthesis of glass powders in the BaO Al_2O_3 SiO_2 system. J Noncryst Solids 100:278 283

27. Lee I, Covino J (1994) Sol gel synthesis of monoclinic phase of barium aluminosilicate ceramics. Mater Res Bull 29:55 62

28. Makishima A, Nagata T (1988) Application of the sol gel pro cess to lower the melting temperature of glaze. J Noncryst Solids 100:519 522

29. Puig J, Ansart F, Lenormand P, Antoine L, Dailly J (2011) Sol gel synthesis and characterization of barium (magnesium) alu minosilicate glass sealants for solid oxide fuel cells. J Noncryst Solids 357:3490 3494

30. Gross SM, Koppitz T, Remmel J, Bouche JB, Reisgen U (2006) Joining properties of a composite glass ceramic sealant. Fuel Cells Bull 9:12 15

31. Payao JC, Schmidt W, Schroeder G (2000) Fundamentos de ensaio de vazamento e estanqueidade. Forschungszentrum Juelich GmbH, Jülich

32. Bansal NP, Gamble EA (2005) Crystallization kinetics of a solid oxide fuel cell seal glass by differential thermal analysis. J Power Sources 147:107 115

33. Sun T, Xiao H, Guo W, Hong X (2010) Effect of Al_2O_3 content on BaO Al_2O_3 B_2O_3 SiO_2 glass sealant for solid oxide fuel cell. Ceram Int 36:821 826

34. Geasee P, Schwickert T, Diekmann U, Conradt R (2001) In: Heinrich JG, Aldinger F (eds) Ceramic materials and components for engines. Wiley, Weinheim, Germany, pp 57 62

35. Lara C, Pascual MJ, Keding R, Duran A (2006) Electrical behaviour of glass ceramics in the systems RO BaO SiO_2 (R Mg, Zn) for sealing SOFCs. J Power Sources 157:377 384